

# Elucidating appealing features of differentiable auto-correlation functions: a study on the modified exponential kernel

Matthias G.R. Faes<sup>a,b,d</sup>, Matteo Broggi<sup>d</sup>, Pol D. Spanos<sup>c</sup>, Michael Beer<sup>d,e,f</sup>

<sup>a</sup>*TU Dortmund University, Chair for Reliability Engineering, Leonard-Euler Straße 5, 44227 Dortmund, Germany*

<sup>b</sup>*KU Leuven, Jan De Nayerlaan 5, 2860 Sint-Katelijne-Waver, Belgium. Email: matthias.faes@kuleuven.be*

<sup>c</sup>*Rice University, 232 Mechanical Engineering Building, Houston, TX, United States*

<sup>d</sup>*Institute for Risk and Reliability, Leibniz Universität Hannover, Callinstr. 34, 30167 Hannover, Germany*

<sup>e</sup>*Institute for Risk and Uncertainty and School of Engineering, University of Liverpool, Peach Street, Liverpool L69 7ZF, UK*

<sup>f</sup>*International Joint Research Center for Engineering Reliability and Stochastic Mechanics, Tongji University, 1239 Siping Road, Shanghai 200092, P.R. China*

---

## Abstract

Research on stochastic processes in recent decades has pointed out that, in the context of modelling spatial or temporal uncertainties, auto-correlation functions that are differentiable at the origin have advantages over functions that are not differentiable. For instance, the non-differentiability of e.g., single exponential auto-correlation functions yields non-smooth sample paths. Such sample paths might not be physically possible or may yield numerical difficulties when used as random parameters in partial differential equations (such as encountered in e.g., mechanical equilibrium problems). Further, it is known that due to the non-differentiability of certain auto-correlation functions, more terms are required in the series expansion representations of the associated stochastic processes. This makes these representations less efficient from a computational standpoint.

This paper elucidates some additional appealing features of auto-correlation functions which are differentiable at the origin. Further, it focuses on enhancing the arguments in favor of these functions already available in literature. Specifically, attention is placed on single exponential, modified exponential and squared exponential auto-correlation functions, which can be shown to be all part of the Whittle-Matérn family of functions. To start, it is shown that the power spectrum of differentiable kernels converges faster to zero with increasing frequency as compared to non-differentiable ones. This property allows capturing the same percentage of the total energy of the spectrum with a smaller cut-off frequency, and hence, less stochastic terms in the harmonic representation of stochastic processes. Further, this point is examined with regards to the Karhunen-Loève series expansion and first and second order Markov processes, generated by auto-regressive representations. The need for finite differentiability is stressed and illustrated.

*Keywords:*

## 23 1. Introduction

24 Many of the loads on engineering components, structures, and systems, as well as the constitutive  
25 properties of these assets exhibit a stochastic nature. This assertion is based on the observation that these  
26 quantities exhibit apparent variability in time and/or space. In this context, the theoretical framework  
27 of stochastic process, and by extension, of random fields [19] has proven an excellent means for capturing  
28 inherent (aleatory) uncertainty [6]. Stochastic processes represent in essence jointly distributed random  
29 variables whose correlation function depends on time and/or space. Throughout literature, efficient meth-  
30 ods have been introduced to effectively and accurately sample from these potentially high-dimensional  
31 joint distributions.

32 Typically, the auto-correlation of such stochastic process is governed by a pre-defined auto-correlation  
33 function (also often referred to as ‘kernel’). This function describes the correlation between two random  
34 variables in the stochastic process as a function of the distance in time/space between them. Alterna-  
35 tively, in case the process is stationary, the auto-correlation is governed by the relative distance between  
36 two points. This paper focuses on auto-correlation functions that belong to the Whittle-Matérn family of  
37 functions. Special attention is given to the single exponential, modified exponential and squared exponen-  
38 tial auto-correlation functions. The generation of samples from these stochastic processes is usually done  
39 using the well-known Karhunen-Loève series expansion [13, 21] or the spectral representation method as  
40 introduced by [7], [8] and later by [6]. Also extended versions of these techniques have been introduced.  
41 Examples of such methods include the Stochastic Harmonic Function representation by [1].

42 The single exponential auto-correlation kernel has been used extensively in engineering applications.  
43 For instance, [5] applied this kernel to represent a stochastic process to model the permeability in resin  
44 transfer molding simulation. Further, in [3], Bayesian updating in a geo-technical context was done based  
45 on a single exponential kernel. In fact, the overview paper of [4] shows that the single exponential model  
46 is most popular in geotechnical engineering, with a total of 47% of examined papers reporting usage  
47 of this auto-correlation model. The single exponential kernel is often selected due to the availability of  
48 analytical solutions to the eigenvalue problem corresponding to the Karhunen-Loève series expansion.  
49 However, the appropriate selection of the auto-correlation function is of large importance for the correct  
50 modelling and simulation of the phenomenon or property under consideration.

51 More relevantly to the problem discussed herein, [2] studied the effect of the auto-correlation function  
52 on the probability of failure in several geo-technical examples. In this work, the authors showed that the  
53 smoothness of a sample path had a significant effect on the probability of failure. This is particularly true  
54 when no spatial averaging is present in the considered problem capable of smoothing out local variations.  
55 Further, it was shown that the sample path smoothness depends on the functional form of the auto-

56 correlation function, and, more precisely, on the differentiability of such function at zero-lag. Thus, this  
57 work clearly illustrated that the auto-correlation function ends up affecting the probability of failure.

58 Furthermore in this context, [18] noted that the application of the single exponential auto-correlation  
59 kernel tends to underestimate the failure risk in the unsaturated slope risk assessment. In addition, they  
60 pointed out how the differentiability of the auto-correlation function affects the truncation order of the  
61 Karhunen-Loève series expansion. Also in this regard, [14] showed that square exponential kernels are  
62 preferable over single exponential kernels, allowing for a highly exact series expansion representation with  
63 far fewer terms in the expansion. Similar observations were made by [15] in the context of modelling  
64 stochastic ocean waves. In essence, they showed that fewer stochastic variables are required to describe  
65 stochastic processes with a narrow spectral bandwidth (i.e., spectra that converge relatively fast to zero  
66 away from the “central” frequency). A comprehensive study of the convergence of second order statistics  
67 of KL-simulated stochastic processes in function of the correlation length, functional form of the auto-  
68 correlation function and solution method is given by [22], indicating similar conclusions. However, the  
69 modified exponential kernel is not studied in this paper.

70 As a final note to this overview of the wide-spread application of single exponential kernels (versus  
71 less frequently used kernels), examination of the literature showed that non-differentiable auto-correlation  
72 functions are used to represent a random ‘stiffness’ term in partial differential equations. To address this,  
73 in [16] the “modified exponential kernel” was introduced to alleviate the shortcomings of the traditional  
74 single exponential kernel caused by non-differentiability. Further, this kernel maintains the enticing prop-  
75 erties of the single exponential kernel, such as the availability of analytical solutions and the possibility to  
76 characterize quickly varying spatial or temporal phenomena. Also, this kernel is more efficient in terms  
77 of the required number of stochastic quantities as compared to the single exponential kernel. These prop-  
78 erties are obtained by addressing the issue of non-differentiability at zero-lag in the single exponential  
79 kernel, while maintaining its functional form to a great extent.

80 This paper builds upon the work that was presented in [16] in three ways. First, it provides additional  
81 explanations of why this particular kernel is highly effective by analytically deriving the energy error  
82 rate convergence in the frequency domain. Second, it compares the modified exponential kernel to  
83 another widely used auto-correlation kernel, namely the squared exponential kernel. Finally, it provides  
84 additional numerical evidence for the effectiveness of the modified exponential kernel in conjunction with  
85 the Karhunen-Loève series expansion, and auto-regressive model representations. The paper is structured  
86 as follows. Section 2 starts by introducing some basic concepts related to the modelling and simulation of  
87 stochastic processes. Section 3 discusses the convergence of the considered auto-correlation kernels both  
88 in the frequency and time domain and discusses the implications hereof for numerical analysis purposes.

89 Finally, Section 4 briefly comprises the conclusions that can be drawn from this work.

## 90 2. Spectral stochastic process representation

### 91 2.1. Definition and stochastic properties

92 A finite-dimensional stochastic process  $f(\mathbf{t}, \theta)$  describes a set of correlated random variables  $f(\theta)$  that  
 93 are assigned to a countable number of locations  $\mathbf{t} \in \Omega$  in the model domain  $\Omega \subset \mathbb{R}^d$  with dimension  $d \in \mathbb{N}$ .  
 94 Each such a random variable  $f(\theta) : (\Theta, \varsigma, P) \mapsto \mathbb{R}$ , with  $\theta \in \Theta$  a coordinate in sample space  $\Theta$  and  $\varsigma$  the  
 95 sigma-algebra, as such maps from a complete probability space to the real domain. This map holds as  
 96 long as  $f(\mathbf{t}, \theta) \in \mathcal{L}^2(\Theta, P)$ , with  $L^2(\Theta, P)$  the Hilbert space of second-order random variables (i.e., finite  
 97 variance). For a given event  $\theta_i \in \Theta$ ,  $f(\mathbf{t}, \theta_i)$  is a realization of the stochastic process. A stochastic process  
 98 is considered Gaussian if the distribution of  $(f(\mathbf{t}_1, \theta), f(\mathbf{t}_2, \theta), \dots, f(\mathbf{t}_n, \theta))$  is jointly Gaussian  $\forall \mathbf{t} \in \Omega$ .

99 Consider  $f(t, \theta)$  to be a zero-mean one-dimensional univariate stochastic process (i.e.,  $\Omega \subset \mathbb{R}$ ) with  
 100 constant variance over the domain and auto-correlation function  $R_{ff}(t, \tau) : \Omega \times \Omega \mapsto [0, 1]$  and  $\tau \subset \Omega$   
 101 a lag parameter. The auto-correlation  $R_{ff}(t, \tau)$  of such a stochastic process represents the correlation  
 102 between two random variables  $f(t, \theta)$  and  $f(t + \tau, \theta)$ , separated by a lag  $\tau$ . That is,

$$R_{ff}(t, \tau) = \frac{CV[f(t, \theta)f(t + \tau, \theta)]}{\sqrt{V[f(t, \theta)]}\sqrt{V[f(t + \tau, \theta)]}}, \quad (1)$$

103 with  $CV[\cdot, \cdot]$  denoting an operator that returns the covariance and  $V[\cdot]$  an operator returning the variance  
 104 of the argument. In this regard,  $\tau$  may represent a distance in time or space. In the remainder of this  
 105 paper, only homogeneous auto-correlation functions, i.e.,  $R_{ff}(\tau)$  are considered.

106 In practical applications, often analytical models for the auto-correlation are applied [2]. In this  
 107 context, particularly the auto-correlation functions belonging to the family of Whittle-Matérn type of  
 108 functions are popular, the formulation of which is given as:

$$R_{ff}^\nu(\tau) = \frac{2^{1-\nu}}{\Gamma(\nu)} \left(\sqrt{2\nu}\frac{\tau}{b}\right)^\nu K_\nu\left(\sqrt{2\nu}\frac{\tau}{b}\right), \quad (2)$$

109 where  $\nu$  is the so-called “smoothness” parameter,  $\Gamma$  denotes the Gamma function,  $K_\nu$  is the modified  
 110 Bessel function of the second kind and  $b$  is the correlation length. It can be shown that for  $\nu = p + 0.5$ ,  
 111 with  $p \in \mathbb{N}^+$ , the Whittle-Matérn correlation function family can be represented as the product of an  
 112 exponential and of a polynomial of order  $p$ . That is,

$$R_{ff}^{p+0.5}(\tau) = \exp\left(-\frac{\sqrt{2p+1}\tau}{b}\right) \frac{p!}{(2p)!} \sum_{i=1}^p \frac{(p+i)!}{i!(p-i)!} \left(\frac{2\sqrt{2p+1}\tau}{b}\right)^{p-i}. \quad (3)$$

113 From this equation, it is straightforward to show that the cases of  $p = 0$ ,  $p = 1$  and  $p \rightarrow \infty$  give  
 114 rise to the so-called single exponential, modified exponential and squared exponential auto-correlation  
 115 functions. Namely, the single exponential auto-correlation function is given as

$$R_{ff}^{0.5}(\tau) = \exp(-|\tau|/b); \quad (4)$$

116 the modified exponential auto-correlation function [16] is given as

$$R_{ff}^{1.5}(\tau) = \exp(-|\tau|/b)(1 + |\tau|/b); \quad (5)$$

117 and the squared-exponential auto-correlation function is given as

$$R_{ff}^{\infty}(\tau) = \exp(-\tau^2/b^2). \quad (6)$$

118 As a final note, it is worthy to mention that the sample paths of a Gaussian process with a Whittle-  
 119 Matérn kernel are  $[\nu] - 1$  times differentiable. In the available literature, single and squared exponential  
 120 functions are commonly used in various application domains. As discussed in [2], the main difference  
 121 between these two auto-correlation functions is the smoothness of the resulting sample paths; related  
 122 applications to soil engineering can be found in references such as [9] and [10]. The main advantage  
 123 of a single exponential kernel is the availability of analytical solutions in terms of its Karhunen-Loève  
 124 expansion [20], and the capability to characterize quickly varying phenomena. However, it exhibits non-  
 125 differentiability at zero-lag, which causes non-differentiable sample paths (i.e.,  $C - 0$  continuity).

126 On the other hand, the squared exponential provides infinitely differentiable sample paths, but does  
 127 not provide analytical solution for the terms of the expansion. Further, as Stein [11] argues, the infinite  
 128 differentiability yields unrealistic results for physical processes, since observing only a small continuous  
 129 fraction of space/time should, in theory, yield the whole process sample [11]. It should be pointed out,  
 130 that for all practical reasons, a Whittle-Matérn function with  $p = 3.5$  can be considered to be *almost*  
 131 equal to  $p \rightarrow \infty$  [12].

132 The modified exponential auto-correlation function aims at combining the strengths of both the afore-  
 133 mentioned kernels, as it provides the temporal/geometric characteristics of the sample paths of a single  
 134 exponential kernel, it solves the problem of the zero-lag discontinuities, and it provides analytical solu-  
 135 tions for its Karhunen-Loève expansion [16]. Further, for many physical processes arising in mechanical  
 136 or civil engineering, first-order differentiability is sufficient, as for instance illustrated in [10] in the case  
 137 of soil mechanics. For instance, taking a practical standpoint, when considering certain input quan-  
 138 tities to a Finite Element model in a quasi-static context, no higher-order differentiability due to the

139 approximations of the functional solution spaces made. In this context, note that Gaussian processes  
 140 that are governed by a Whittle-Matérn kernel are  $\lceil \nu \rceil - 1$  times differentiable in a mean-square sense [17].  
 141 This property makes this family of auto-correlation functions particularly appealing to model physical  
 142 processes in a realistic and mathematically rigorous way.

143 Alternatively, the auto-correlation of  $(f(t_1, \theta), f(t_2, \theta), \dots, f(t_n, \theta))$  can be represented in the fre-  
 144 quency domain by means of a two-sided power spectrum  $S_{ff}(\omega) : \Gamma \times \Gamma \mapsto \mathbb{R}$ , with  $\Gamma \subset \mathbb{R}$  the frequency  
 145 domain. The Wiener-Khintchine theorem allows for the calculation of the auto-correlation function  
 146  $R_{ff}(\tau)$  of a stochastic process from its two-sided power spectrum  $S_{ff}(\omega)$  and vice versa based on the  
 147 following Fourier transforms:

$$S_{ff}(\omega) = \frac{1}{2\pi} \int_{-\infty}^{+\infty} R_{ff}(\tau) e^{-i\omega\tau} d\tau, \quad (7)$$

148 and

$$R_{ff}(\tau) = \int_{-\infty}^{+\infty} S_{ff}(\omega) e^{i\omega\tau} d\omega. \quad (8)$$

149 Applying the Wiener-Khintchine theorem to the auto-correlation function defined in Eq. (2) yields  
 150 the form

$$S_{ff}^\nu(\omega) = \frac{2\pi^{0.5}\Gamma(\nu + 0.5)(2\nu)^\nu}{\Gamma(\nu)b^{2\nu}} \left( \frac{2\nu}{b^2} + 4\pi^2\omega^2 \right)^{-\nu+0.5} \quad (9)$$

151 for the corresponding power spectrum.

152 The power spectra corresponding to the auto-correlation functions in Eqs. 4–6 can be similarly shown  
 153 to be given by the equations

$$S_{ff}^{0.5}(\omega) = \frac{1}{\pi} \frac{b}{b^2\omega^2 + 1}, \quad (10)$$

$$S_{ff}^{1.5}(\omega) = \frac{1}{\pi} \frac{2b}{(b^2\omega^2 + 1)^2}, \quad (11)$$

155 and

$$S_{ff}^\infty(\omega) = \frac{1b}{2\sqrt{\pi}} \exp \frac{-b^2\omega^2}{4}. \quad (12)$$

156 Close inspection of Eq. (9) reveals that the “smoothness” parameter, which is also critical for the  
 157 differentiability of  $R_{ff}^\nu$  for  $\tau \rightarrow 0$ , determines the range over which the energy content of the spectrum  
 158 is spread out. Indeed, since  $\nu$  determines the order of the denominator, it affects the rate with which  
 159  $S_{ff}^\nu(\omega)$  tends to 0 for increasing  $\omega$  values. Take for instance the case of Eq. 10. It is clear that in this  
 160 case, due to the lack of higher order terms in the denominator, the energy content is broadly distributed  
 161 over  $\omega$ . Similarly, it can be seen that the energy content of the modified exponential kernel decreases  
 162 quadratically with respect to the term  $b^2\omega^2 + 1$  in Eq. 11. As such, the bandwidth of the single exponential  
 163 kernel is wider as compared to the modified exponential. Finally, the  $\exp(\cdot)$  term in Eq. 12 suggests that

164 most of the energy content is located in the lower frequencies for the squared exponential kernel. Thus,  
 165 it is shown that the power-spectra of the zero-lag differentiable kernels, i.e., the modified and squared  
 166 exponential kernel, converge faster to zero as  $\omega \rightarrow \infty$ .

## 167 2.2. Simulation of stochastic processes

### 168 2.2.1. Spectral representation

169 Following the power spectral representation of the auto-correlation of a stochastic process, the simu-  
 170 lation of paths of this process can be done according to [7, 6] using the equation

$$f(t, \theta) = \sqrt{2} \sum_{n=0}^{N-1} A_n \cos(\omega_n t + \psi_n(\theta)), \quad (13)$$

171 where

$$A_n = \sqrt{2S_{ff}(\omega_n)\Delta\omega}, \quad (14)$$

172 and  $\omega_n$  is defined as

$$\omega_n = n\Delta\omega, \quad (15)$$

173 where  $n = 1, \dots, N-1$  and  $\Delta\omega = \omega_u/N$ . The phase angles  $\psi_n(\theta)$  are considered random and distributed  
 174 as  $\mathcal{U}(0, 2\pi)$ , with  $\mathcal{U}$  the uniform distribution. Thus, samples  $f(t, \theta_i)$  of the stochastic process can be  
 175 generated by sampling from  $\mathcal{U}(0, 2\pi)$ . The parameter  $\omega_u$  represents the cut-off frequency, beyond which  
 176 the power spectral density function  $S_{ff}(\omega)$  may be assumed to be zero for either mathematical or physical  
 177 reasons. In practice, an energy criterion is commonly used. That is,

$$\int_0^{\omega_u} S_{ff}(\omega_n) d\omega = (1 - e_S) \int_0^{\infty} S_{ff}(\omega_n) d\omega, \quad (16)$$

178 with  $e_S$  a measure for the error, which is typically a small value, e.g.,  $e_S = 0.01$  or  $e_S = 0.001$ . In  
 179 this regard, the appropriate selection of  $\omega_u$  is important for the accuracy of the analysis. In essence, it  
 180 represents the degree of approximation of the energy content used in the representation of the stochastic  
 181 process. As such, if  $\omega_u$  is selected too small, a significant fraction of the energy of the modelled signal is  
 182 lost. This might lead to an underestimation of the magnitude of the physical quantity under consideration,  
 183 which can lead to severe limitations, e.g., underestimation of probability of failure. Further,  $\omega_u$  cannot  
 184 be selected arbitrarily larger for numerical reasons. Specifically, extremely high values of  $\omega_u$  require a  
 185 corresponding quite high number of random variables  $\psi_n(\theta)$ , leading to computationally costly procedures.  
 186 Further, note that while herein attention is focused on the spectral representation, these arguments are  
 187 also pertinent to other simulation methods based in the frequency domain, e.g., the Stochastic Harmonic

188 Function representation [1].

### 189 2.2.2. Karhunen-Loève expansion

190 The Karhunen-Loève expansion is a potent tool for representing stochastic processes [20]. Specifically,  
 191 following the Karhunen-Loève (KL) series expansion, a stochastic process  $f(t, \theta)$  is represented as:

$$f(t, \theta) = \mu_x(t) + \sigma_f \sum_{i=1}^{\infty} \sqrt{\lambda_i} \psi_i(t) \xi_i(\theta), \quad (17)$$

192 where  $\sigma_f$  is the standard deviation of the random field. The quantities  $\lambda_i \in (0, \infty)$  and  $\psi_i(t) : \Omega \mapsto \mathbb{R}$  are  
 193 respectively the eigenvalues and eigenfunctions of the continuous, bounded, symmetric and positive (semi-  
 194 ) definite auto-correlation function  $R_{ff}(\tau)$ . The decomposition of  $R_{ff}(\tau)$  is performed in accordance with  
 195 Mercer's theorem. That is,

$$R_{ff}(\tau) = \sum_{i=1}^{\infty} \lambda_i \psi_i(t) \psi_i(t'). \quad (18)$$

196 These quantities are in practice obtained by solving the homogeneous Fredholm integral equation of  
 197 the second kind. That is,

$$\int_{\Omega} R_{ff}(\tau) \psi_i(t') dt' = \lambda_i \psi_i(t), \quad (19)$$

198 with  $t' = t + \tau$ . Analytical solutions to this equation exist only for a limited number of auto-correlation  
 199 functions. In general, discretization schemes are used to solve this equation, as explained in [21]. Since  
 200  $R_{ff}(\tau)$  is bounded, symmetric, positive semi-definite, and, in most practical cases, can be even assumed  
 201 positive definite, the eigenvalues  $\lambda_i$  are non-negative and the eigenfunctions  $\psi_i(t)$  satisfy the orthogonality  
 202 condition

$$\langle \psi_i(t), \psi_j(t) \rangle = \int_{\Omega} \psi_i(t) \psi_j(t) dt = \delta_{ij}, \quad (20)$$

203 with  $\delta_{ij}$  the Kronecker delta.  $\langle \cdot, \cdot \rangle : \Omega \times \Omega \mapsto \mathbb{R}$  denotes the inner product in the functional space. Hence,  
 204 the eigenfunctions form a complete orthogonal basis on an  $\mathcal{L}_2$  Hilbert space. In this case, the series  
 205 expansion in Eq. 18 can be shown to be optimally convergent [20].

206 For practical reasons, the infinite series expansion in Eq. 17 must be truncated after a finite number  
 207 of terms  $n_{KL} \in \mathbb{N}$ . That is,

$$f(t, \theta) = \sigma_f \sum_{i=1}^{n_{KL}} \sqrt{\lambda_i} \psi_i(t) \xi_i(\theta), \quad (21)$$

208 where  $n_{KL}$  should be selected such that following inequality holds:

$$1 - \frac{1}{|\Omega|} \frac{1}{\sigma_f^2} \sum_{i=1}^{n_{KL}} \lambda_i \leq e_{\sigma}, \quad (22)$$



209 with  $e_\sigma$  the so-called mean error variance [21] and  $|\Omega|$  denoting the length of the simulation domain.

210 In contrast to  $e_S$  introduced in Eq. (16), the quantity  $e_\sigma$  does not represent some sort of energy loss  
 211 measure. Instead,  $e_\sigma$  represents the percentage of the variance of the original process that is captured by  
 212 the truncated Karhunen-Loève expansion. In this respect, if  $n_{KL}$  is selected too small, it will lead to a loss  
 213 of the variance in the representation. Hence, the magnitude of the physical quantity under consideration  
 214 will be underestimated. Finally, similarly to the spectral representation, setting  $n_{KL}$  too large will  
 215 render the computational cost of the corresponding analysis untractable due to the high dimension of the  
 216 parameter input space.

### 217 2.2.3. Auto-regressive models

218 A third commonly used approach to simulate stochastic processes and fields is the auto-regressive  
 219 representation (AR) method [23]. According to the AR framework, the value of a stochastic process  
 220  $f(t, \theta)$  at time  $t_k$  with order  $m$  can be computed as

$$f(t_k, \theta) = - \sum_{i=1}^m a_i f(t_{k-i}) + b_0 w(t_k, \theta), \quad (23)$$

221 where  $a_i$  are the AR parameters and  $b_0$  is the gain factor of the AR model.  $w(t_k)$  is a band limited  
 222  $[-\omega_b, \omega_b]$  white-noise process that satisfies

$$E [w(t_k)w(t_l)^T] = 2\omega_b I_n \delta_{kl}, \quad (24)$$

223 where  $E[\bullet]$  and  $\bullet^T$  denotes the operators of mathematical expectation and transpose respectively,  $\omega_b$  is  
 224 the cut-off frequency,  $I_n$  is the identity matrix and  $\delta_{kl}$  the Kronecker delta. The representation in Eq. (23)  
 225 is the best linear estimator of  $f(t_k, \theta)$  by using the  $m$  previous values  $[f(t_k), f(t_{k-1}), \dots, f(t_{k-m})]$ . The  
 226 corresponding error  $\epsilon$  can be expressed as:

$$\epsilon = \frac{\Delta t}{2\pi} E \left[ \left( f(t_k, \theta) + \sum_{i=1}^m a_i f(t_{k-i}) \right) \right] = b_0^2. \quad (25)$$

227 The parameters  $a_i$  in the series expansion defined in Eq. (23) can generally be determined by minimiz-  
 228 ing  $\epsilon$ . This leads to the so-called Yule-Walker equations that relate the stationary target auto-correlation  
 229 function  $R_{ff}(\tau) \equiv R_{ff}(t_k - t_i)$  to the AR parameters via a Toeplitz system of equations:

$$\sum_{i=1}^m R_{ff}(t_k - t_i) a_i = -R_{ff}(t_k) \quad k = 1, \dots, m \quad (26)$$

230 Alternative approaches used to fit an AR model to a predefined auto-correlation model interpret

Eq. (23) as the response of a discrete linear system to a white-noise excitation. For a thorough explanation of the fitting of an AR model to a predefined auto-correlation function or power spectral density, the reader is referred to the work of [23] or [24].

### 3. Convergence of the stochastic process representations

In this section analytical expressions are derived for the energy approximation error of the spectral stochastic representation of the three considered auto-correlation kernels. Then, the paper provides additional illustrations regarding the improved convergence behavior of the modified exponential kernel over the single exponential when they are used in the context of a KL expansion. Finally, a comparison of AR models for these three auto-correlation functions is included for the sake of completeness.

#### 3.1. Spectral stochastic representation

The convergence behavior of the auto-correlation functions in Eqs. 4-6 is studied with respect to Eq. 16. In this context, analytical expressions for the approximation error  $e_s$  are derived with respect to the cut-off frequency  $\omega_u$ . Note that similar expressions can be derived for all members of the Whittle-Matérn class of auto-correlation functions that abide  $\nu = p + 0.5$ . A general expression of the error in function of  $\nu$  is far from trivial to obtain and falls outside the scope of this paper. To determine the cut-off frequency  $\omega_u$  using Eq. (16), the power spectra  $S_{ff}(\omega)$  in Eqs. 10-12 needs to be integrated. The right hand side integral of  $S_{ff}(\omega)$  w.r.t.  $\omega$  is obtained by means of substitution and given for these power spectra by the equations

$$\int_0^\infty S_{ff}^{0.5}(\omega)d\omega = \left[ \frac{1}{\pi} \tan^{-1}(b\omega) \right]_0^\infty = \frac{1}{2}, \quad (27)$$

$$\int_0^\infty S_{ff}^{1.5}(\omega)d\omega = \left[ \frac{1}{\pi} 4b \left( \frac{\omega}{2(\omega^2 b^2 + 1)} + \frac{1}{2b} \tan^{-1}(b\omega) \right) \right]_0^\infty = 1, \quad (28)$$

and

$$\int_0^\infty S_{ff}^\infty(\omega)d\omega = \left[ \operatorname{erf} \left( \frac{b\omega}{2} \right) \right]_0^\infty = 1, \quad (29)$$

where  $\operatorname{erf}(x) = \frac{1}{\sqrt{\pi}} \int_0^x e^{-t^2} dt$  is the error function.

Similarly, the left-hand side of Eq. (16) for the considered auto-correlation functions can be determined as

$$\begin{aligned} \int_0^{\omega_u} S_{ff}^{0.5}(\omega)d\omega &= \left[ \frac{1}{\pi} \tan^{-1}(b\omega) \right]_0^{\omega_u} \\ &= \frac{1}{\pi} \tan^{-1}(b\omega_u), \end{aligned} \quad (30)$$

$$\begin{aligned} \int_0^{\omega_u} S_{ff}^{1.5}(\omega) d\omega &= \left[ \frac{1}{\pi} 4b \left( \frac{\omega}{2(\omega^2 b^2 + 1)} + \frac{1}{2b} \tan^{-1}(b\omega) \right) \right]_0^{\omega_u} \\ &= \frac{1}{\pi} 4b \left( \frac{\omega_u}{2(\omega_u^2 b^2 + 1)} + \frac{1}{2b} \tan^{-1}(b\omega_u) \right), \end{aligned} \quad (31)$$

255 and

$$\begin{aligned} \int_0^{\omega_u} S_{ff}^{\infty}(\omega) d\omega &= \left[ \operatorname{erf} \left( \frac{b\omega}{2} \right) \right]_0^{\omega_u} \\ &= \operatorname{erf} \left( \frac{b\omega_u}{2} \right). \end{aligned} \quad (32)$$

256 Using these equations in conjunction with Eq. (16), and isolating the desired truncation error  $e_S$   
257 provides relations between the error and the cut-off frequency  $\omega_u$ . Specifically,

$$e_{S,0.5} = 1 - \frac{2}{\pi} \tan^{-1}(b\omega_u), \quad (33)$$

258

$$e_{S,1.5} = 1 - \frac{2}{\pi} \left( \frac{b\omega_u}{b^2\omega_u^2 + 1} + \tan^{-1}(b\omega_u) \right), \quad (34)$$

259 and

$$e_{S,\infty} = 1 - \operatorname{erf} \left( \omega_u \frac{b}{2} \right). \quad (35)$$

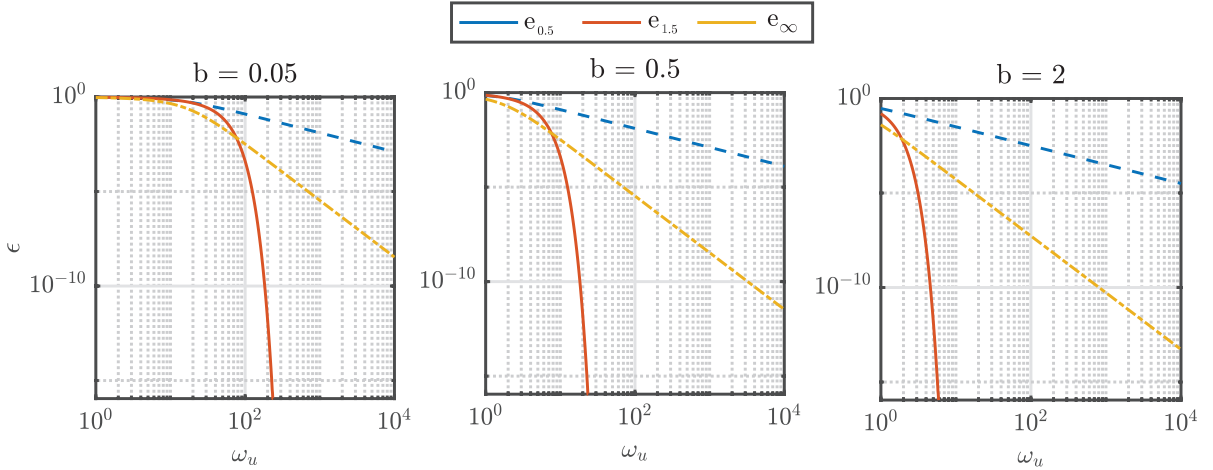


Figure 1: Decay of the energy approximation error  $e$  as a function of the truncation frequency  $\omega_u$ . Plots for different values of the correlation length  $b$  are given.

260 Figure 1 shows the decay of the truncation error of the energy  $e_S$  as a function of the selected  $\omega_u$  for the  
261 considered auto-correlation models, for several different values of the correlation lengths  $b = [0.05, 0.5, 2]$ .  
262 The decay function is calculated according to Eq. (33) to (35). In particular, a zero-mean Gaussian  
263 stochastic process with unit variance on a domain  $t \in [0, 5]$  is considered for this purpose. From this

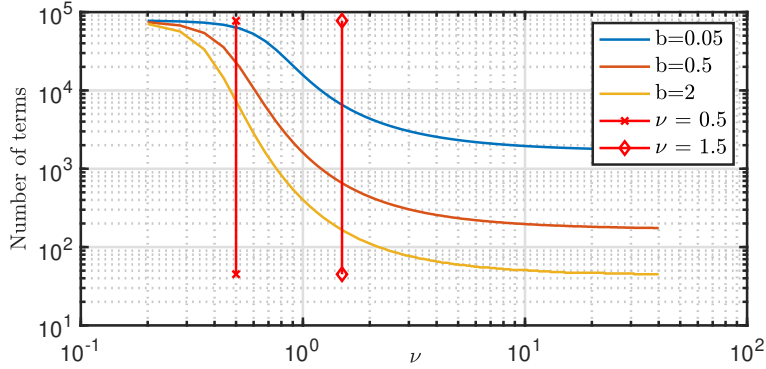


Figure 2: Number of terms in the spectral expansion as a function of the smoothness parameter of the Matérn kernel.

264 Figure, it is clear that this approximation error decays significantly faster in squared and modified  
 265 exponential kernels as compared to a single exponential kernel. Specifically, the squared exponential  
 266 kernel converges super-linearly, the modified exponential kernel converges linearly with a slope of 2.13  
 267 and the single exponential kernel converges linearly with a slope of 0.87. These findings are valid for  
 268 all correlation lengths tested. The difference in the convergence rate between the modified and the  
 269 single exponential kernels originates from the  $\frac{b\omega_u}{b^2\omega_u^2+1}$ -term in Eq. (34). This term ensures that the error  
 270 for the modified exponential kernel decreases faster versus the single exponential case when  $w_u \rightarrow \infty$ .  
 271 Nevertheless, note that the shape of the decay of the error with respect to  $\omega_u$  is similar for both single  
 272 and modified exponential curves.

273 These considerations are further elucidated in Figure 2, which shows the number of terms in the  
 274 spectral expansion (see also Eq. (13)) that are required to represent 99.9% of the energy of the power  
 275 spectrum. Also from this figure, it is clear that higher  $\nu$  values and hence, a higher-order differentiability  
 276 of the auto-correlation function at zero lag, yields more efficient representations of the random field. It  
 277 is furthermore clear that the number of terms converges after approx.  $\nu = 10$ .

278 In Figure 3 sample paths of the corresponding Gaussian stochastic processes are shown for different  
 279 values of the truncation error  $e_S$ . Each sample path is created with all the three correlation structures in  
 280 the time  $t \in [0, 5]$ , but only  $t \in [0, 0.1]$  is shown to better visualize the local characteristic of the samples.  
 281 This Figure shows how the sample path from the exponential correlation exhibits non-negligible high  
 282 frequency oscillations and noise when compared with the other two correlations when lower values of  
 283  $e_S$  are used. This is a direct result of the slower convergence of the single exponential kernel in energy  
 284 content, which in its turn is related to the non-differentiability of  $R_{ff}$  at zero lag. As pointed out in the  
 285 literature, these high-frequency oscillations potentially impact the engineering analysis affected by the  
 286 properties modeled with this kernel.

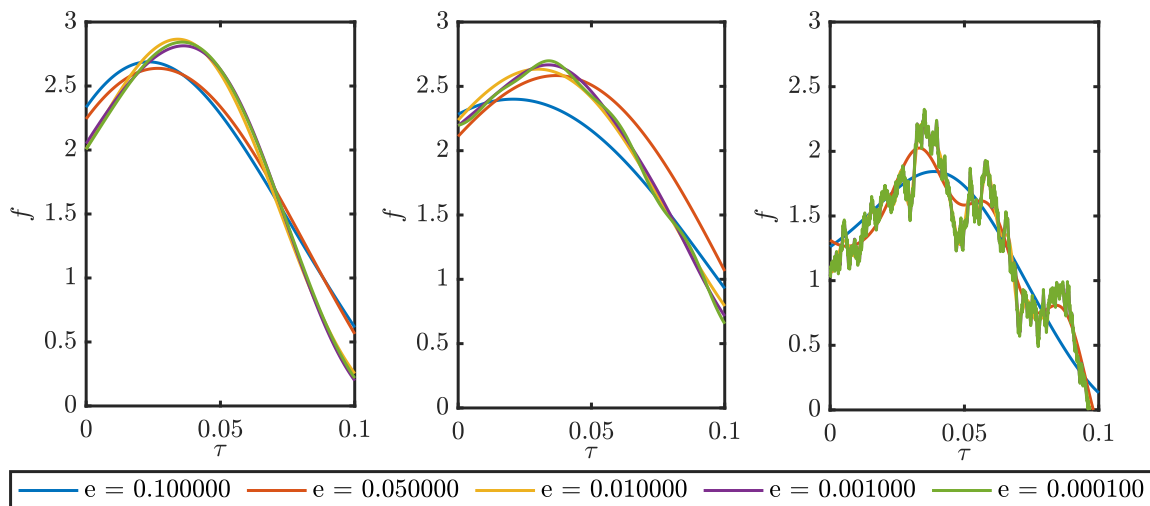


Figure 3: Sample paths of a one-dimensional Gaussian stochastic process, where the auto-correlation is governed by a Squared exponential (left), Modified exponential (middle) and Single exponential (right) kernel function, for different values of the truncation error.

### 287 3.2. Karhunen-Loève expansion

288 The advantage of using the modified exponential kernel over a single exponential one in terms of  
 289 required terms in the Karhunen-Loève expansion has been illustrated in [16]. In this section, additional  
 290 insights into this topic are attempted. In particular, it is shown that the reduction in the requisite number  
 291 of stochastic terms holds consistently for the entire process series expansion. Further, this property also  
 292 holds for a wide range of correlation length values. Figure 4 shows the convergence of the mean error  
 293 variance as a function of the number of terms that are retained in the KL expansion for the same  
 294 stochastic process considered in Section 3.1. Herein, the solution of the Fredholm integral equation in  
 295 Eq. 19 is obtained using a Galerkin procedure with Legendre basis functions. Clearly, the convergence  
 296 of the mean error variance corresponding to the squared exponential process is the fastest of the three  
 297 considered auto-correlation functions. These results further confirm the findings of [16], namely that the  
 298 modified exponential kernel converges faster than the single exponential kernel when considering the KL  
 299 expansion for a wide range of correlation length values. This can be also explained by the differentiability  
 300 of the auto-correlation function at zero-lag.

### 301 3.3. AR model representation

302 For the study of the applicability of the considered auto-correlation functions in conjunction with an  
 303 AR representation, an analytical approach is used. In particular, the required AR models are derived  
 304 based on the considered auto-correlation functions.

305 Regarding the single exponential covariance kernel  $R_{ff}^{0.5}(\tau)$ , it can be shown that an AR(1) process,  
 306 i.e., an AR process with  $m = 1$  is capable of directly representing a Gaussian process with  $R_{ff}^{0.5}(\tau)$  [19].

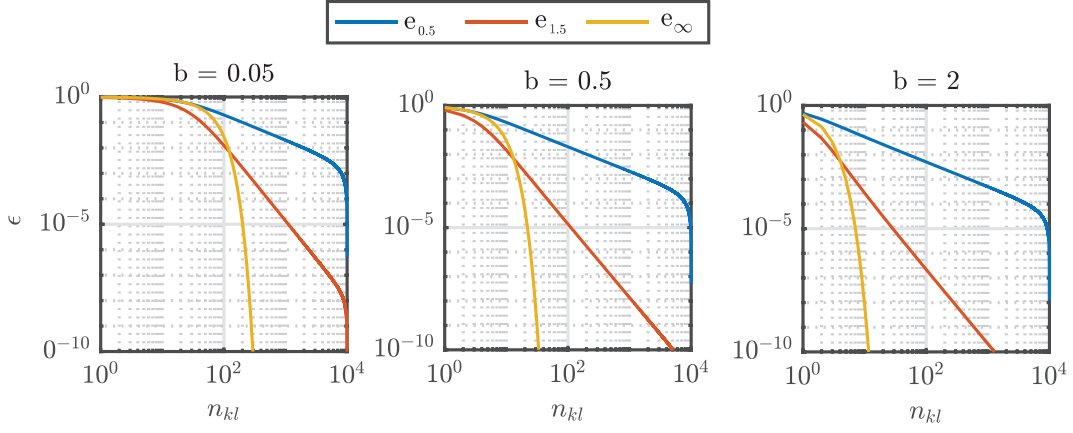


Figure 4: Convergence of the mean error variance with respect to the number of terms in the KL Expansion for the three considered auto-correlation kernels.

307 To capture this, write out Eq. (23) for  $m = 1$  and subtract  $f(t, \theta)$  from both sides. That is,

$$[f(t + 1, \theta) - f(t, \theta)] + (1 - a)f(t, \theta) = b_0 w(t, \theta). \quad (36)$$

308 The associated first-order differential equation to this finite-difference equation is

$$\frac{d}{dt} f(t, \theta) + \alpha f(t, \theta) = b_0 w(t, \theta), \quad (37)$$

309 which can be interpreted as a linear model that links  $f(t, \theta)$  to a white-noise excitation. In the limit state  
310 for infinitesimally small  $\tau$ , the transfer function corresponding to Eq.(37) is

$$H(\omega) = \frac{1}{i\omega + \alpha}, \quad (38)$$

311 that in combination with a constant spectral density  $S_0$  gives rise to the power spectral density  $S_{ff}(\omega)$ :

$$S_{ff}(\omega) = \frac{S_0}{\omega^2 + \alpha^2}, \quad (39)$$

312 for  $f(, \omega)$ . This can be related through Eq. (8) to the auto-correlation function:

$$R_{ff}(\tau) = 1 \exp(-|\tau|\alpha), \quad (40)$$

313 which corresponds to a single exponential auto-correlation function.

314 Following a similar procedure, it can be shown that an AR(1) model of the following form:

$$f(t, \theta) = a [f(t - 1, \theta) + f(t + 1, \theta)] + b_0 w(t, \theta) \quad (41)$$

315 corresponds to a stationary Gaussian process with power spectral density:

$$S_{ff}(\omega) = \frac{4\alpha^3}{\pi(\omega^2 + \alpha^2)^2}, \quad (42)$$

316 and hence with auto correlation function

$$R_{ff}(\tau) = \exp(-\alpha|\tau|)(\alpha|\tau| + 1), \quad (43)$$

317 that corresponds to the modified exponential kernel. For the squared exponential auto-correlation func-  
318 tion, a one-on-one exact relationship with a corresponding AR model is not trivial to establish and  
319 requires the solution of the Yule-Walker equations. This falls outside the scope of this paper.

#### 320 4. Concluding remarks

321 In this paper, certain aspects relating to the mathematical behavior of common auto-correlation  
322 functions have been studied. Specifically, the convergence of the spectral density of the process to zero  
323 as the frequency tends to infinity has been examined. In particular, attention has been focussed on  
324 the comparison of the spectral convergence of functions that are differentiable at zero-lag versus those  
325 that are not-differentiable. In this regard, some selected functions from the Whittle-Matérn family were  
326 considered: the exponential, modified exponential and squared exponential function. This family has the  
327 appealing feature that the differentiability of the sample-paths is tuneable by tuning the differentiability  
328 of the auto-correlation function. The most popular member of this family is the single exponential  
329 auto-correlation function due to the availability of analytical solutions. However, as explained, the  
330 resulting sample paths are non-differentiable and the convergence of the stochastic representation is  
331 comparatively slow when compared to other functions. Of this family of auto-correlation functions, the  
332 squared exponential auto-correlation function was found to be the most efficient in terms of convergence  
333 properties. However, both the lack of analytical solutions, as the infinite differentiability of the sample  
334 paths make its application questionable from an application and physical standpoint.

335 It has been shown, both analytically and numerically, that the number of stochastic components  
336 required to represent a stochastic process with the single exponential kernel is considerably larger when  
337 compared to a modified or squared exponential kernel. This statement holds for both stochastic spectral  
338 representation methods, as well as for the well-known Karhunen-Loève series expansion. In this con-  
339 text, note that the single exponential kernel is not differentiable at zero lag, whereas, the modified and  
340 squared exponential kernel are completely differentiable. Squared exponential auto-correlation functions  
341 on the other hand show the fastest convergence. However, their infinite differentiability poses impor-

342 tant limitations with respect to their physical interpretation. It is found that auto-correlations from the  
343 Whittle-Matérn family with half-integer values pose an interesting trade-off between efficiency and phys-  
344 ical interpretability. Of this family, the so-called modified exponential auto-correlation function stands  
345 out due to the availability of analytical solutions to the Fredholm integral equation of the second kind.

346 Further, in the paper AR models have been considered, for which it has been shown that for both a  
347 single and modified exponential kernel, a closed form expression for an AR(1) model can be derived. This  
348 proves that AR models are highly suited to represent these types of stochastic processes. Further work  
349 beyond this initial study can explore the relationship between the differentiability of the auto-correlation  
350 function at zero lag, and the convergence of the corresponding spectral density to zero as the frequency  
351 tends to infinity.

## 352 **Acknowledgments**

353 Matthias Faes acknowledges the support of the Research Foundation Flanders (FWO) under grant  
354 12P3419N, as well as from the Alexander von Humboldt foundation for the partial funding of this work.

## 355 **References**

- 356 [1] J. Chen, W. Sun, J. Li, and J. Xu. Stochastic harmonic function representation of stochastic processes.  
357 *Journal of Applied Mechanics, Transactions ASME*, 80(1) (2013), 1–11.
- 358 [2] J. Ching and K.-K. Phoon, Impact of auto-correlation Function Model on the Probability of Failure.  
359 *Journal of Engineering Mechanics*, 145:04018123, 2018.
- 360 [3] Z. Cao and Y. Wang, Bayesian model comparison and selection of spatial correlation functions for soil  
361 parameters. *Structural Safety*, 49:10–17, 2014.
- 362 [4] Cami, B., Javankhoshdel, S., Phoon, K. K. and Ching, J. Y. Scale of Fluctuation for Spatially Varying  
363 Soils: Estimation Methods and Values. *ASCE-ASME Journal of Risk and Uncertainty in Engineering*  
364 *Systems, Part A: Civil Engineering*, 6(4), 03120002, 2020.
- 365 [5] F. Desplentere, I. Verpoest and S. Lomov, Stochastic flow modeling for resin transfer moulding. *AIP*  
366 *Conference Proceedings*, 1152:284–292, 2009.
- 367 [6] M. Shinozuka and G. Deodatis, Simulation of Stochastic Processes by Spectral Representation.  
368 *Applied Mechanics Reviews*, 44:191—204, 1991.
- 369 [7] S.O. Rice, "Mathematical Analysis of Random Noise" in Selected Papers of Noise and Stochastic  
370 Processes, Edited by N. Wax, Dover Publications, Inc, New York, 1954, pp. 180- 18



- 371 [8] L.E. Borgman, "Ocean Wave Simulation for Engineering Design," Journal of Waterways and Harbor  
372 Div., ASCE, Vol. No. WW4, November, 1969, pp. 557- 583.
- 373 [9] Q. Yue, J. Yao, A. H-S Ang, P D. Spanos. Efficient random field modeling of soil deposits properties.  
374 Soil Dynamics and Earthquake Engineering, 108: 1-12, 2018.
- 375 [10] Q. Yue and J. Yao. Soil deposit stochastic settlement simulation using an improved auto-correlation  
376 model. Probabilistic Engineering Mechanics, 59, 103038, 2020.
- 377 [11] M.L. Stein. Interpolation of spatial data: some theory for Kriging. Springer Science & Business  
378 Media, 2012.
- 379 [12] Chang, Y. C., Ching, J. Y., Phoon, K. K. and Q. X., Yue. On the Hole Effect in Soil Spatial  
380 Variability. *ASCE-ASME Journal of Risk and Uncertainty in Engineering Systems, Part A: Civil*  
381 *Engineering*, 7(4), 04021039, 2021.
- 382 [13] G. Stefanou & M. Papadrakakis. Assessment of spectral representation and Karhunen-Loève expan-  
383 sion methods for the simulation of Gaussian stochastic fields. *Computer Methods in Applied Mechanics*  
384 *and Engineering*, 196(21–24) (2007), 2465–2477.
- 385 [14] B. Sudret & A. Der Kiureghian (2000). Stochastic finite element methods and reliability. A state-  
386 of-the-art-report. In Technical Rep. UCB/SEMM-2000/08, Univ. of California, Berkeley, CA (Issue  
387 November).
- 388 [15] P.D. Sclavounos (2012). Karhunen–Loève representation of stochastic ocean waves. *Proceedings of*  
389 *the Royal Society A: Mathematical, Physical and Engineering Sciences*, 468(2145), 2574–2594.
- 390 [16] P. Spanos, M. Beer and J. Red-Horse, Karhunen–Loève Expansion of Stochastic Processes with a  
391 Modified Exponential Covariance Kernel. *Journal of Engineering Mechanics*, 133:773–779, 2007.
- 392 [17] Rasmussen, Carl Edward and Williams C.K.I. Gaussian processes in machine learning. Summer  
393 school on machine learning. Springer, Berlin, Heidelberg, 2003.
- 394 [18] L. Wang, C. Wu, Y. Li, H. Liu, W. Zhang and X. Chen, Probabilistic Risk Assessment of unsatu-  
395 rated Slope Failure Considering Spatial Variability of Hydraulic Parameters. *KSCE Journal of Civil*  
396 *Engineering*, 23(12):5032–5040, 2019.
- 397 [19] E. Vanmarcke, *Random Fields: Analysis and Synthesis*, MIT Press, Cambridge, 1983.
- 398 [20] P. Spanos, R. Ghanem, Stochastic finite element expansion for random media, *Journal of engineering*  
399 *mechanics* 115 (5) (1989) 1035–1053.

- 400 [21] W. Betz, I. Papaioannou, D. Straub, Numerical methods for the discretization of random fields by  
401 means of the Karhunen-Loève expansion, *Computer Methods in Applied Mechanics and Engineering*  
402 271 (2014) 109–129.
- 403 [22] S. P. Huang, S. T. Quek, K. K. Phoon, Convergence study of the truncated Karhunen–Loève expan-  
404 sion for simulation of stochastic processes, *International Journal for Numerical Methods in Engineering*  
405 52 (9) (2001) 1029–1043.
- 406 [23] P. D. Spanos, B. A. Zeldin. Efficient Iterative Arma Approximation of Multivariate Random Pro-  
407 cesses For Structural Dynamics Applications. *Earthquake Engineering And Structural Dynamics*, 25  
408 (1996), 497–507.
- 409 [24] P.D. Spanos, B. A. Zeldin. Monte Carlo treatment of random fields: A broad perspective. *Applied*  
410 *Mechanics Reviews*, 51 (1998), 219-237
- 411 [25] Hewer, Rüdiger, et al. A Matérn-based multivariate Gaussian random process for a consistent model  
412 of the horizontal wind components and related variables. *Journal of the Atmospheric Sciences* 74.11  
413 (2017), 3833-3845.